A FLUID STRUCTURE COUPLING OF THE ARIANE-5 DURING START PHASE BY DES

Heinrich Lüdeke and Javier B. Calvo

German Aerospace Center, Institute of Aerodynamics and Flow Technology, Lilienthalplatz 7, D-38108 Braunschweig

ABSTRACT

Concerning the requirements of future rocket technologies, which are the cost-efficient access to orbit as well as an increase in system reliability, a deeper insight into the unsteady phenomena during ascent of modern launchers is essential. Especially unsteady interactions and resonances of flow separation inside the nozzle, the turbulent launcher wake and the nozzle structure play an important role for the design of future main stage propulsion systems. The so called buffeting coupling phenomenon is one of the main challenges during ascent. In the present study of the Ariane-5 launcher a coupled simulation of the afterbody with a realistic structural and aerodynamic representation of different nozzle configurations is carried out using unsteady Detached Eddy Simulations on the CFD side, coupled with second order structural computations for different nozzle configurations. The essential features of the interaction process are well captured.

Key words: DES; bufeting coupling; Ariane; Nozzle.

1. INTRODUCTION

Concerning requirements of future launcher technologies, the rocket engine is one of the most important parts. A deeper insight into the unsteady phenomena in the nozzle region during the start phase and especially unsteady side-loads, induced by the interaction of flow separation in the launcher wake and the nozzle structure will play an important role for the design of future propulsion systems. This so called buffeting coupling is still one of the main challenges during ascent. In the last decade various experimental and numerical studies have been carried out concerning the ascent of the Ariane-5 launcher. The coupling between external pressure pulsations and internal shock position was investigated for example by Torngren [1]. Structural ovalization modes of simplified nozzle configurations and influences of forced nozzle motions at given frequencies on the dynamics of shock waves inside the nozzle are taken into account by Schwane [2]. However until now it was not possible to simulate the unsteady turbulent flow field of the whole launcher configuration and the interaction with the realistic nozzle structure simultaneously by hybrid LES/RANS methods. DES, as proposed by Spalart et.al. [3], is expected as a promising approach to resolve the unsteady turbulent flow field of such configurations as shown by Deck [4]. DES is a hybrid approach for the modelling of turbulent flow fields at complex geometries by combining the best features of Reynolds-averaged Navier-Stokes (RANS) in boundary layers and the large eddy simulation (LES) outside to predict massively separated unsteady flow fields at high Reynolds-numbers especially in separated wake flows. In various numerical studies over the last years steady and unsteady turbulent simulations of the Ariane-5 configuration were carried out under turbulent transonic conditions with and without plume [5]. The DES results were compared with experimental data of the FFA T1500 wind tunnel facility of the FOI Sweden. After these flow-field investigations fluid structure couplings are carried out for the nozzle part to investigate resonance phenomena and loads. In a first step this is tested using the geometry of the wind tunnel model nozzle with the transferred structure of the Vulcain-2 nozzle and finally with the realistic geometry of the Vulcain-2 for the whole coupling cycle. A typical Mach number field for the configuration, including nozzle flow and plume is shown in Fig. 1. In former investigations steady and unsteady Ariane-5 simulations under turbulent conditions are carried out at transonic wind tunnel conditions including jet flow and launcher wake [6]. While in the first studies simplified generic configurations of the launcher were investigated, here unstructured grids are generated including heliumshell, connectors between booster and main body as well as various other details and two different nozzle geometries. Fig. 2 gives an impression of the details the NLR model, used for wind tunnel testing. After preliminary coupled simulations with a simplified structural description of the nozzle [5], a structural description as well as a CFD grid of the Vulcain-2 nozzle contour is used. The structural representation of the nozzle is provided by EADS-ST. The FEM computations of the structure are carried out by the commercial tool ANSYS [5] and the coupling by interpolation routines of the Technical University Braunschweig [7] and the commercial MPCCI library [5].

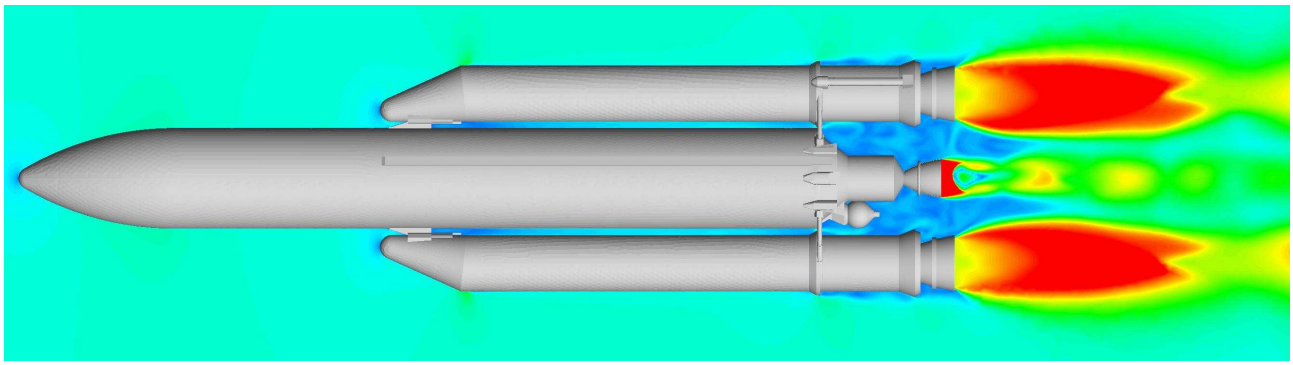

Figure 1. Mach number contours of the Ariane-5 launcher at $M_\infty = 0.8$. Steady RANS simulation

2. NUMERICAL SIMULATION TOOLS

2.1. CFD-solver TAU

The CFD computations for this study are performed by the hybrid structured/unstructured DLR Navier-Stokes Solver TAU [8]. The DLR-TAU-code is a second order finite-volume flow solver for the Euler and Navier-Stokes equations in the integral form. Different numerical schemes like cell-centered for sub- and transonic flow and AUSMDV for super- and hypersonic flow conditions are implemented. Second-order accuracy for upwind schemes is obtained by the MUSCL extrapolation, in order to allow the capturing of strong shocks and contact discontinuities. A three-stage explicit Runge-Kutta scheme as well as a point implicit LUSGS scheme are options to advance the solutions in time for steady flow fields. For convergence acceleration local time stepping, implicit residual smoothing and full multigrid are implemented. Fast and accurate transient flow simulations are computed by a second order Jameson type dual time stepping scheme, as an implicit algorithm which is not restricted in the choice of the smallest time step in the flow field. Several one- and two equation turbulence models are available for steady as well as unsteady simulations. In the presented RANS-cases the one-equation Spalart-Allmaras (SA) model is used which is briefly described in the following. The model defines the eddy viscosity field as

$$\mu_t = \rho\nu_t = \rho\tilde{\nu} f_{\nu 1} \tag{1}$$

with ρ as the density, ν_t as the turbulent kinematic viscosity and $f_{\nu 1}$ as a near wall-function that guarantees linear behavior of the turbulent transport quantity in the vicinity of walls:

$$f_{\nu 1} = \left(\frac{\chi^3}{\chi^3 + c_{\nu 1}^3} \right), \; \chi = \frac{\tilde{\nu}}{\nu} \tag{2}$$

with ν as the molecular viscosity. The distribution of the transport quantity $\tilde{\nu}$ is determined by the solution of

$$\frac{D(\rho\tilde{\nu})}{Dt} = \underbrace{c_{b1}\tilde{S}\rho\tilde{\nu}}_{P} - \underbrace{c_{w1} f_w \rho \left(\frac{\tilde{\nu}}{d}\right)^2}_{D} + \underbrace{\frac{\rho}{\sigma}\left\{\nabla\left[(\nu+\tilde{\nu})\nabla\tilde{\nu}\right] + c_{b2}(\nabla\tilde{\nu})^2\right\}}_{DF} \tag{3}$$

with d as the wall distance. This transport equation contains phenomenological models of production P, destruction D and diffusion DF. The destruction term D is needed to model the blocking effects near walls. In the production term P a modified vorticity $\tilde{S}$ appears that maintains the linear behavior of the model near walls:

$$\tilde{S} = S + \frac{\tilde{\nu}}{k^2 d^2} f_{\nu 2}, \quad f_{\nu 2} = 1 - \frac{\chi}{1 + \chi f_{\nu 1}} \tag{4}$$

The function $f_{\nu 2}$ is constructed in a way that the vorticity S maintains its log-layer behavior all the way to the wall. The destruction term

$$D = c_{w1} f_w \rho \left(\frac{\tilde{\nu}}{d}\right)^2 \tag{5}$$

is constructed by using the wall function f_w:

$$\begin{aligned} f_w &= g\left[\frac{1 + c_{w3}^6}{g^6 + c_{w3}^6}\right]^{1/6} \\ g &= r + c_{w2}\left(r^6 - r\right) \\ r &= \frac{\tilde{\nu}}{\tilde{S} k^2 d^2} \end{aligned} \tag{6}$$

Figure 2. NLR wind tunnel model for buffeting forces measurements (figure from Maseland [10])

The different model constants $c_{\nu 1}, c_{b1}, c_{b2}, c_{w1}, c_{w3}$ are determined by experimental data and analytical solutions and are well known for turbulent flow fields [9].
During the last decade more recent turbulence models like DES are implemented [3]. DES is a hybrid RANS-LES approach that bases on a modification of the wall distance term in the SA model. While RANS is used in the unsteady boundary layer flow with a standard grid resolution where it performs reasonable results, LES is used in separated regions where relevant turbulent scales can be modeled. The switching between RANS and LES bases on a characteristic length scale, chosen to be proportional with Δ which is the largest cell dimension:

$$\Delta = max(\Delta x, \Delta y, \Delta z) \tag{7}$$

For the standard DES formulation the wall distance d in the SA model is replaced by $\tilde{d}$ which is defined as:

$$\tilde{d} = min(d, C_{DES}\Delta) \tag{8}$$

with C_{DES} as a constant calibrated by using isotropic turbulence. Outside of the boundary layer a local equilibrium between production and destruction term in the SA model is expected. This local balance leads to the relation $\tilde{\nu} \propto \tilde{S} \cdot \tilde{d}^2$ which is very similar to the relation in the Smagorinsky model, namely $\nu_t \propto S \cdot d^2$.

2.2. Fluid-Structure coupling

The equation which governs the structural dynamics in an unsteady Finite Element model [11] is

$$[M]\{\ddot{q}(t)\} + [C]\{\dot{q}(t)\} + [K]\{q(t)\} = \{R(t)\} \tag{9}$$

with R(t) as the aerodynamic forces, q(t) as the nodal displacement vector, $\dot{q}(t)$ as the nodal velocity vector and $\ddot{q}(t)$ as the nodal acceleration vector. Three matrices are taken into account, named by $[M]$ for the mass matrix, $[C]$ for the damping matrix and $[K]$ for the stiffness matrix. In our analysis, the applied external load is only given by the forces inside and outside of the nozzle. A strong loose coupling scheme is used to obtain a solution of the problem. The software in which the algorithm is implemented has been and is being developed within Integrated design of the Hot Structures (IMENS+) DLR project. Each of the coprocesses sets the boundary conditions, starts, stops, and controls a simulation code. The physical quantities are exchanged by means of conservative extended VTK interpolation routines [7] or optionally by commercial MPCCI routines. The coprocesses and the exchange of the physical quantities are controlled by a python script called control code, in which the coupling scheme is implemented. Within this software, a strong coupled solution algorithm is used. The flux diagram of the program is shown in Fig. 3. It contains two loops, an inner and an outer loop. In the inner loop, we obtain a solution within the time interval $[t_n, t_{n+1}]$ by means of an equilibrium iteration and using the reduction of deformations as a convergence criterion. In the outer

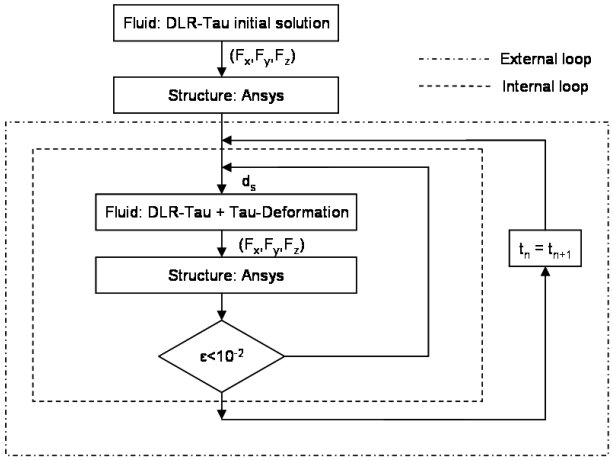

Figure 3. Flux diagram of the coupling procedure

loop, the time of the simulation is updated and the program is prepared to compute a new inner loop. The main steps are:

1. The flow solution is read and mean nodal forces are transferred by a conservative interpolation.
2. The forces are used as a boundary condition on each of the structure nodes. Then, the displacement of the structure is obtained for the current time interval $[t_n, t_{n+1}]$ and mapped on the fluid mesh.
3. The fluid mesh is deformed by an additional deformation module according to the given displacements.
4. A new flow solution is calculated, taking into account the movement of the structure .
5. A new structural solution gives the displacement of the structural nodes.
6. The convergence of the internal loop is checked by calculating the total change of deformations($\epsilon \leq 10^{-2}$). If this convergence criterion is not fulfilled, the loop returns to point 3.
7. The current time is updated and the programs returns to point 3.

Normally, within the simulation, at least two equilibrium loops, and between two and four are necessary to achieve the desired convergence.

2.3. Interpolation between structural and aerodynamic part

In order to apply the calculated aerodynamic forces, they have to be transformed to the structural grid points. Since obviously the aerodynamic and structural grids do not coincide, a methodology for the transfer of loads and displacements between the grids has to be employed. The

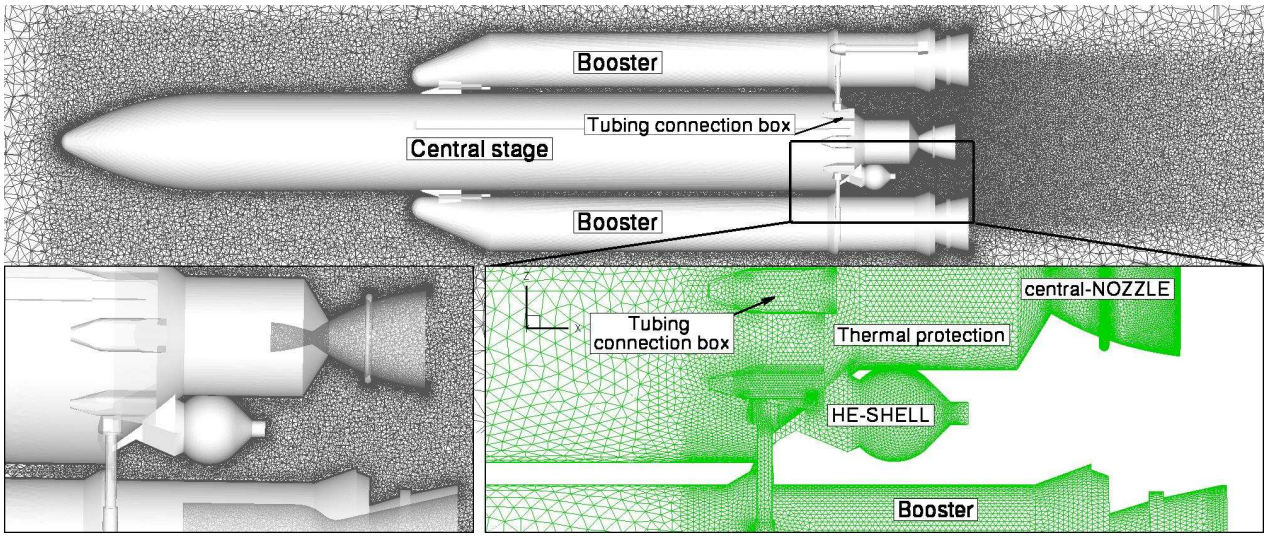

Figure 4. Symmetry plane of the Ariane-5 grid with Vulcain-2 nozzle and cut outs of the nozzle section

software Visualization Tool Kit (VTK) in addition to the necessary modifications and algorithms [7] is used as interpolation routine for the Vulcain 2 grid while for the study of the Volvo-S6 wind tunnel nozzle the commercial MPCCI toolkit was used. A conservative interpolation is chosen for the analysis because both the structure and the fluid are solved unsteadily [12]. The advantage of the conservative formulation lies in the higher numerical accuracy as well as in the physical justification for the transfer of forces and displacements between different surface discretizations. This approach was used for the present study and it assures that, within the expected accuracy, no energy is added to the system in the simulation time. At the beginning of the simulation a matrix which maps the inner and outer walls of the nozzle on the nodes of the structural shell elements is computed.

3. COMPUTATIONAL GRIDS

3.1. CFD-grids

While in former studies [6] simplified configurations and nozzle geometries with structured hexahedral grids [13] were investigated, for the presented simulations the whole launcher geometry, provided by FOI [5], was discretized by surface triangles with a strongly increased grid density in the nozzle region and around the helium tank. In an additional step the wind tunnel model geometry is modified by exchanging the central nozzle by the original Vulcain-2 geometry, provided by EADS-ST. Due to the problem of highly time consuming DES simulations all regions without special interest for the buffeting coupling are discretized as coarse as possible to receive a grid with about $6 \cdot 10^6$ nodes totally. Nevertheless this grid contains the whole non symmetric launcher with various details (see Fig. 4). The booster nozzles, which were not included in the CAD description, were designed by following the shape and dimensions of the former grids to resolve the principle experimental setup, where a double sting with outlets was mounted inside [5]. Also the helium tank aside of the central nozzle is modified to provide better grid resolution in the boundary layer by simplifying geometrical constraints. Fuel tubes at the body, included in the wind tunnel model, were omitted with the exception of the fittings at the end that can have significant influence on the nozzle. A detailed view of the nozzle section is included in Fig. 4 to get an overview of the grid resolution between boosters and central Nozzle.

3.2. Ansys-grids

The structural behaviour of the Volvo-S6 and the Vulcain-2 nozzle extension [14] is carried out by using the commercial software Ansys. For the Vulcain-2 geometry a simplified model of the nozzle, which contains its three main parts: tube wall, Turbine Exhaust Gases (TEG), and the outskirt is used in the simulation while the geometry of the Volvo-S6 nozzle is kept unchanged. The simplified models were calibrated to show the same natural frequencies and modes according to the original structural description, provided by EADS-ST. The torus TEG is simplified for the Vulcain-2 grid and is kept uniform as shown in Fig. 5 together with comparisons of the 2^{nd} mode and the Volvo-S6 nozzle. The elements used in Ansys for this configuration are shell elements for the structure and outskirt stiffeners and beam elements for the tube wall stiffeners. The complete Vulcain-2 structural model has 8640 nodes and 9064 elements. The mesh exchanged with the flow solver contains only the shell elements which define the geometry. Thus, the stiffeners are just modelled in the structural part.

4. NUMERICAL RESULTS

4.1. Flow and boundary conditions for Volvo-S6 and Vulcain-2 case

For the calculations of the Ariane-5 nozzle-flowfield, wind tunnel conditions of M=0.8, $Re = 25 \cdot 10^6$ related to the launcher length are chosen [5]. In addition to the Volvo-S6 nozzle of the wind tunnel tests the original shape of the Vulcain-2 nozzle was included to the launcher geometry (See Fig. 4). All computations were carried out under the assumption of perfect gas, also inside of the nozzle since the experiments used high pressure nitrogen for the jets. This is also the reason for the chosen temperature at the nozzle inflow plane of 400 K. For the Volvo-S6 nozzle the chamber pressure was taken from wind tunnel conditions as 4.3 MPa while for the Vulcain-2 geometry the pressure was adapted with respect to the area ratio and the flight conditions to 11.7 MPa.

4.2. Steady RANS-results

DES, as a method for the description of unsteady turbulent flow, needs a steady turbulent solution to start, which is generated with the same RANS model DES bases on. Such a RANS solution for the full configuration at Mach 0.8 is shown in Fig. 1. The interaction between the different plumes and the structures between the boosters and the central nozzle in the symmetry plane can be seen clearly, even for this steady simulation.

4.3. DES Results of the flow field

As a next step towards a coupled transient CSD-CFD simulation Detached Eddy Simulations with both configurations of the Ariane 5 model were started regardless the structural behavior of the nozzle. These computations ran with a physical timestep of $4ms$ (flight time) for about $7s$ for the Vulcain-2 configuration. Due to the supersonic flow conditions in the nozzle plumes the AUSMDV upwind scheme was chosen for the numerics.

DES results of the launcher are shown in Fig. 6,which is a snapshot figure, for the Volvo-S6 and the Vulcain-2 geometry. The flow structures that appear on the main stage nozzle, generated by the vortical flowfield near the edge of the cylindrical part of the central stage are clearly visible. In the right part of Fig. 6 (side view) the influence of the tubing connection box (see Fig. 4) on the stream traces can be seen clearly. A difference in the position of the pressure maximum at the lower part of both nozzles (Fig. 6 both side views) is a direct result of the displacement of the wake vortex separating at the edge of the central stage, also shown in Fig. 7, side view, by the averaged pressure and stream lines. Another important detail of the investigated configuration is the asymmetry of the launcher generated by the helium-shell which is obviously of significant size. Different experimental studies have shown influences of this sphere on the unsteady behavior of the flow on both sides of the central nozzle. A shading effect on the pressure fluctuations in that region where the shell is located was stated in former studies [13] and numerical simulations without this sphere have shown stronger unsteadiness. Nevertheless the mecha-

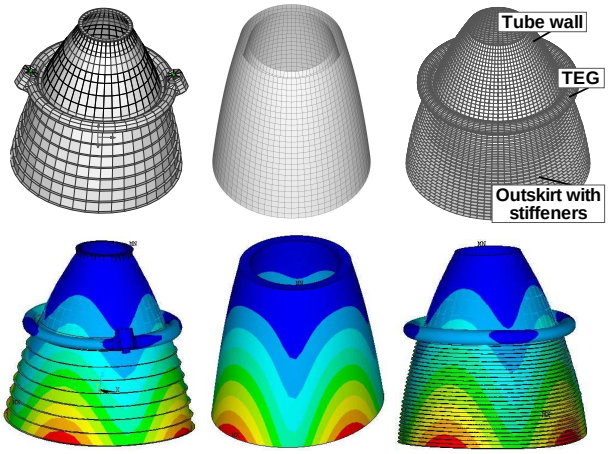

Figure 5. Top: ANSYS structural grids of the Vulcain-2, Volvo-S6 and refined generic Vulcain-2 nozzle for the coupled simulation.Bottom: 2^{nd} modes of the respective structure.

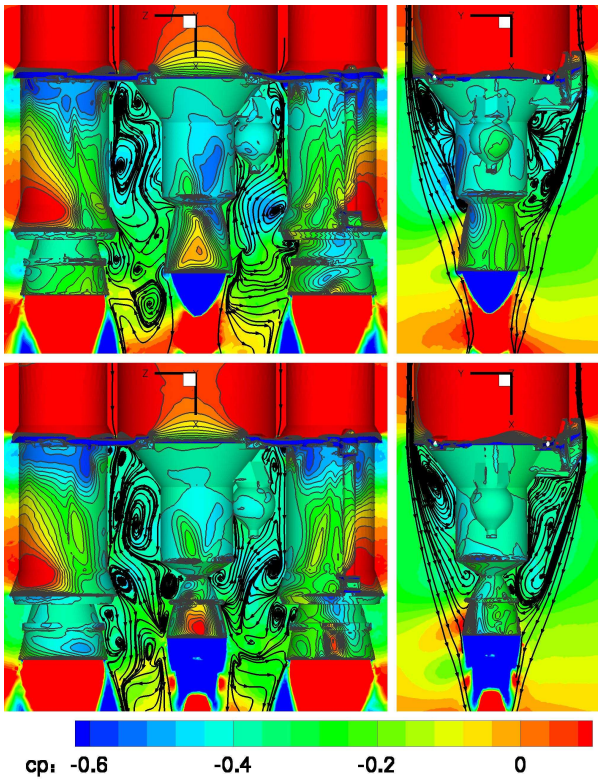

Figure 6. Snapshot of Cp contours and instantaneous stream traces in the nozzle region. Front (left) and side (right) view. Top: Volvo-S6 nozzle, bottom: Vulcain-2 nozzle.

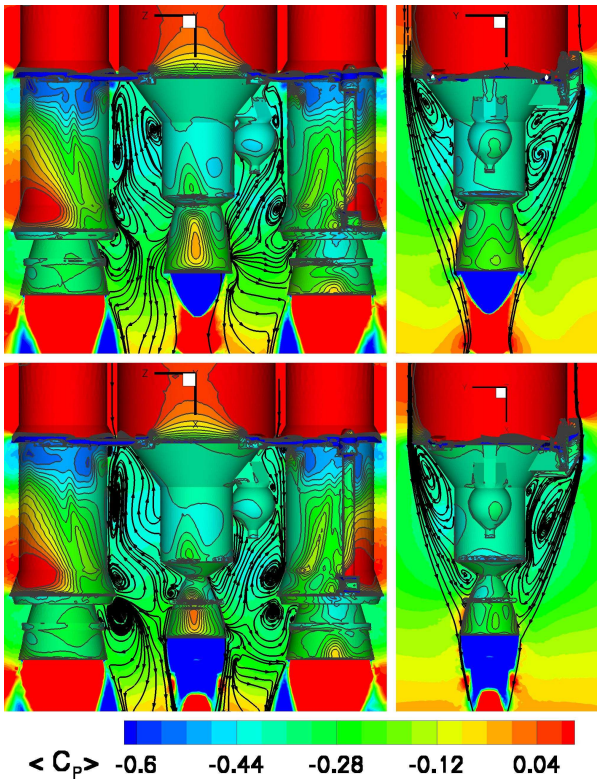

Figure 7. Averaged Cp contours of the configuration and averaged stream traces. Front (left) and side (right) view. Top: Volvo-S6 nozzle, bottom: Vulcain-2 nozzle.

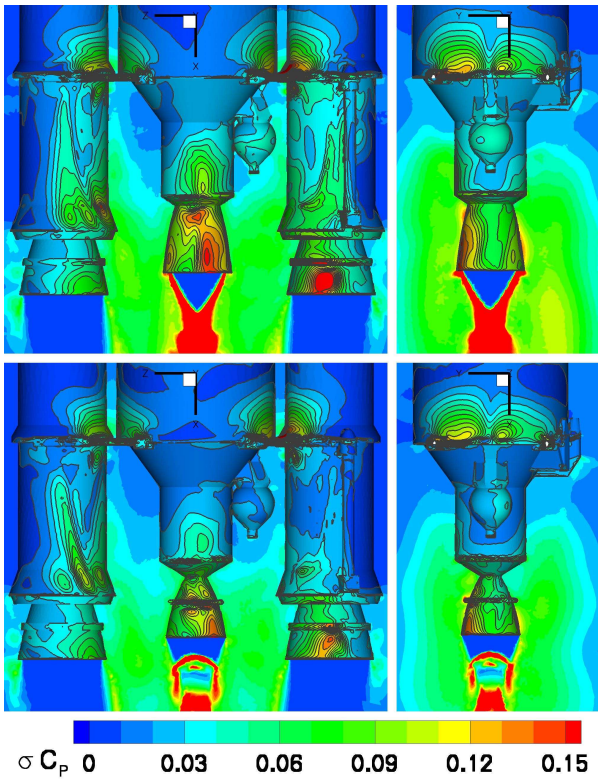

Figure 8. RMS values of unsteady Cp distribution of the configuration. Front(left) and side (right) view. Top: Volvo-S6 nozzle, bottom: Vulcain-2 nozzle.

nisms of the the shading effects are still not fully understood. Even the trace of the pressure contour for the He-shell is visible on the surface aside of the shell. by analyzing the DES-snapshot in Fig. 6 the shading mechanism becomes clear. While in the part without sphere the unsteady flow from the gap between booster and central stage can directly hit the nozzle where a much more refined vortex system develops, this mechanism is blocked by the shell on the opposite side for both configurations.

For a deeper analysis of the results, statistical data was extracted from unsteady simulations in conjunction with the standard deviation of the pressure coefficient, called σCp, which is the Root Mean Square (RMS) value of Cp. A unique feature of all LES and hybrid RANS/LES models like DES is the capability to obtain such RMS-data of the pressure in the whole flow field. In Fig. 8 the regions, where unsteady phenomena appear are characterized by large values of σCp for both nozzle configurations.

An asymmetry of the flow in the nozzle region is visible in the front and side view in Fig. 7 and Fig. 8. While the asymmetry in the front view results from the helium-shell, the already discussed asymmetry in the side view is visibly a consequence of the tubing connection box at the end of the main stage (see Fig. 4). As a result the free shear layer behind the main stage is deflected in a way, that it hits the nozzle at a different position (Fig. 7 side view). This effect appears for both configurations.Aditionally for the Vulcain-2 configuration the nozzle ring (the TEG) influences the flow in this region with respect to the impingement position of the shear layer.

In the experiments an unsteady behavior of the vortex flow was investigated at the lower part of the thermal protection cylinder (on top of the central nozzle, see Fig. 4). This maximum in σCp is clearly visible at the side-view

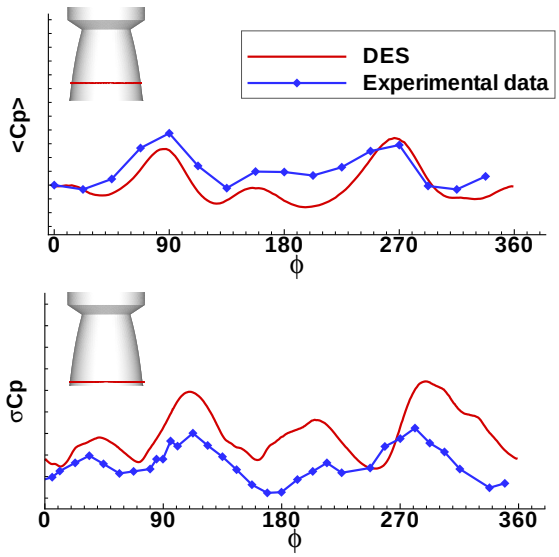

Figure 9. Averaged pressure distribution and standard deviation along circumferental rings around the central nozzle. Comparison between experimental results and DES.

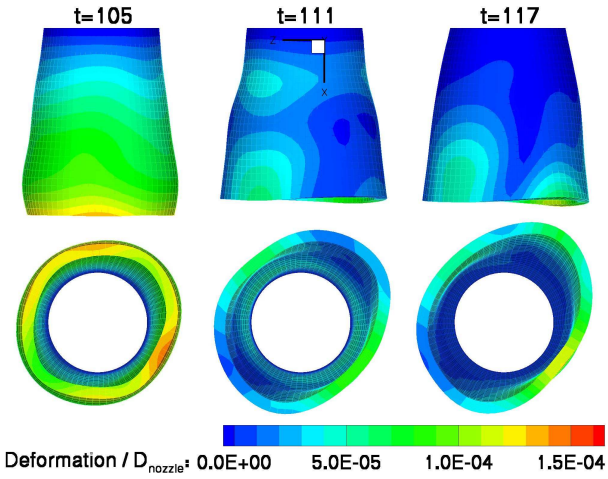

Figure 10. Deformation of the Volvo-S6 nozzle geometry at three dimensionless times, 1000 times exaggerated. Side and bottom view.

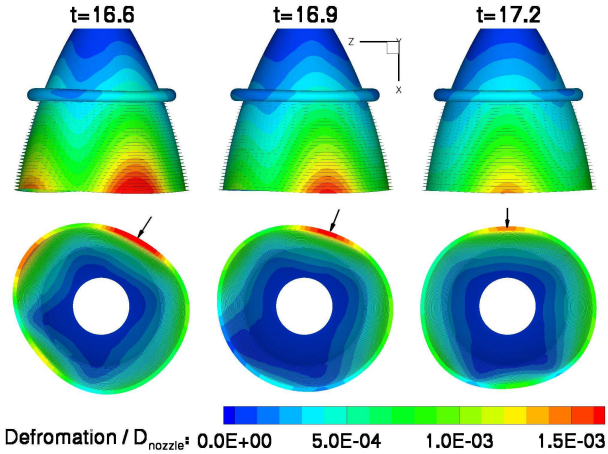

Figure 11. Deformation of the Vulcain-2 nozzle geometry at three dimensionless times, 30 times exaggerated view. Side and bottom view.

of Fig. 8 For a validation of the DES simulations by experimental data, a comparison of Cp and σCp in two respective nozzle cuts is shown in Fig. 9. As visible the angular position of maxima and minima of the wind tunnel data are well fittet by DES, though the RMS-values are globally overpredicted.

4.4. Fluid structure coupling

Finally fluid-structure coupling analysisfor both nozzle geometries were carried out. The computation were performed over several periods of the structural oscillation. At hand of preliminary inviscid simulations on a coarse tetrahedral grid a sufficient physical timestep of $2ms$ in flight time scale for each structural coupling was determined. For both configurations the upper circle of the nozzle structure is fixed while the outflow part is kept free for any deformation. An impression of the computational effort for the coupling can be given by the fact, that each coupling step for the Vulcain-2 configuration took about

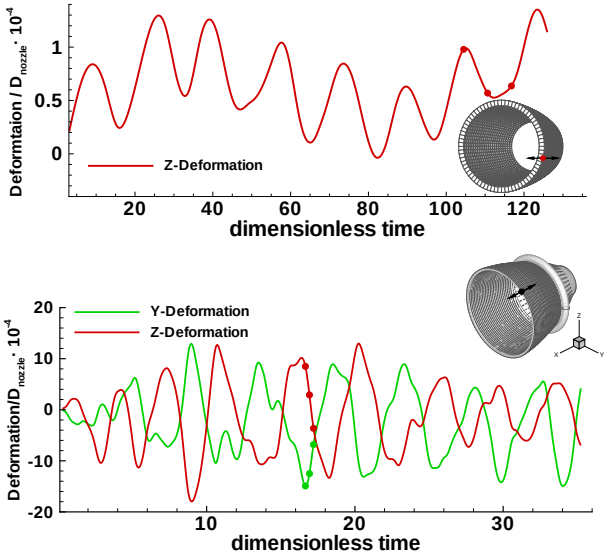

Figure 12. Displacement of a single point on the Volvo-S6 and Vulcain-2 nozzle over dimensionless time.

3 hours of computational time on 128 Blue-Gene processors. A wide spectrum of natural oscillations could be investigated on both nozzle configurations. For the Volvo-S6 nozzle a sequence of 1000 times exaggerated shapes colored by surface deformations is shown in Fig. 10, seen from side and bottom. The view is exxagerated by this factor to give a better impression of the behaviour and the variety of responding structural modes. The deformation contours are scaled by the inner nozzle diameter and the dimensionless time is also scaled by this diameter and the launcher onflow velocity. For the Vulcain-2 nozzle on the other hand mainly an ovalization mode is stimulated superimposed by other modes, resulting in a rotation of the minima and maxima of the deformation (Fig. 11). Such ovalization modes were also investigated by Schwane et. al. [2]. The position of the minimum in the nozzle radius is marked in the bottom view of Fig. 11 by arrows. The couterclockwise rotation of this position is obvious.

In contrast to the Volvo-S6 geometry, where the deformation-amplitude was small compared to the nozzle diameter, this is no longer the case for the realistic Vulcain-2 nozzle simulation where the relative deformation is about 10 times larger. The absolute deformation of the nozzle with an outlet diameter of $2m$ is in the order of $3mm$ in amplitude. In Fig. 12 the relative displacement components of a single point perpendicular to the flow direction are plotted against the dimensionless time used in the former figures. The dimensional resonance frequency of the structure is in the range of 30 Hz, but, as already mentioned, the harmonic movement of this mode is superimposed by additional modes with similar, but not identical frequencies. In addition the timestamps of Fig. 10 and 11 are included as symbols in both curves.

5. CONCLUSIONS

The present study investigates the fluid structure interaction at the nozzle section of the Ariane-5 launcher under transonic conditions. Two nozzle geometries were investigated, a Volvo-S6 nozzle of the wind tunnel model in the FFT 1500 facility and in addition the structure of the Vulcain-2 nozzle. Time accurate Detached Eddy Simulations are performed around the nozzles to resolve most energetic turbulent structures in this area. Furthermore, fluid structure coupling between DES flow simulations and FEM data was carried out and ran over seven periods of nozzle oscillation. The essential interaction between a turbulent flow field and the nozzle structure was demonstrated for the first time for a complete launcher configuration by using hybrid RAS-LES turbulence modelling. For both, the original wind tunnel configuration and a realistic Vulcain-2 nozzle shape, including the structural model, the modal response of different geometries to the unsteady flow field could be investigated in detail. In contrast to simulations for the generic wind tunnel model nozzle, the amplitudes of the Vulcain-2 nozzle deformation lie in a realistic range of the order of $3mm$.

ACKNOWLEDGMENTS

The authors acknowledge EADS-ST for kindly providing the structural data of the Vulcain-2 nozzle and Alexander Filimon for the grid generation during his time as a diploma student at DLR. The coupling software to interpolate CFD onto CSD grids was designed by the Institute for Aircraft Design and Lightweight Structures of the Technical University of Braunschweig. A major part of the study was carried out under the scope of the Pan European infrastructure research programme on High Performance Computing: HPC-Europa. The authors have to acknowledge the EPCC at the University of Edinburgh for their kind assistance and the possibilities to use their Blue-Gene super-computing facility during a grant at their institute, within this program and the University of Glasgow for hosting the author and providing the structural software package during this time.

REFERENCES

[1] Torngren L., Correlation between Outer Flow and Internal Nozzle Pressure Fluctuations, Proceedings of the 4th European Symposium on Aerothermodynamics for Space Vehicles, Capua, Italy 15-18 October (2001)

[2] Schwane R., Xia Y., On the Dynamics of Shock Waves in Over-Expanded Rocket Nozzles, AIAA 2004-1128 (2004)

[3] Spalart P.R., Young-Person's Guide to Detached-Eddy Simulation Grids, NASA/CR-2001-211032, (2001)

[4] Deck S., Thepot R., Thorigny P., Zonal Detached Eddy Simulation of Flow Induced Unsteady Side-Loads over launcher Configurations, 2^{nd} European Conference For Aerospace Sciences, Bussles, Belgium. July 1-6 (2007)

[5] Lüdeke H., Calvo J., Filimon A., Fluid Structure Interaction of the ARIANE-5 Nozzle Section by Advanced Turbulence Models, European Conference on Computational Fluid Dynamics, Egmond aan zee, the Netherlands, September 5-8 (2006)

[6] Lüdeke H., Investigation of the ARIANE-5 Nozzle Section by DES, European Conference for Aerospace Sciences, Moscow, Russia, July 4-7 (2005)

[7] Haupt M., Niesner R., Unger R., Horst P., Computational Aero-Structural Coupling for Hypersonic Applications, AIAA-2006-3252, 9th AIAA/ASME Joint Thermophysics and Heat Transfer Conference, 5-8 June, San Francisco, California (2006)

[8] Mack A., Hannemann V., Validation of the unstructured DLR-TAU-Code for Hypersonic Flows, AIAA 2002-3111, (2002)

[9] Spalart P.R., Allmaras S.R., A One Equation Turbulence Transport Model for Aerodynamic Flows, La Recherche Aerospaciale, **1**, 1994, pp. 5-21 (1994)

[10] Maseland J.E.J., Soemarwoto B.I., Kok J.C., Dynamic Load Predictions for Launchers using Extra-Large Eddy Simulations (X-LES), 5th European Symposium on Aerothermodynamics for Space Vehicles, Cologne, November 8-11 (2004)

[11] Bathe K.J., Finite Element Procedures, Englewood Cliffs, PenticeHall (1996)

[12] Cebral J., Löhner R., Conservative Load Projection and Tracking for Fluid-Structure Interaction Problems, AIAA-97-0797, 34th Aerospace Meeting and Exhibit, Reno, Nevada (1996)

[13] Wong H., Meijer J., Schwane R., Theoretical and Experimental Investigations on Ariane5 Base-Flow Buffeting, 5th European Symposium on Aerothermodynamics for Space Vehicles, Cologne, November 8-11 (2004)

[14] Winterfeldt L., et al., Redesign of the Vulcain 2 Nozzle Extension, AIAA paper 2005-4536 (2005)